PZT Transduction of High-Overtone Contour-Mode Resonators

Hengky Chandrahalim, *Member, IEEE*, Sunil A. Bhave, *Senior Member, IEEE*, Ronald G. Polcawich, *Member, IEEE*, Jeffrey S. Pulskamp, and Roger Kaul, *Senior Life Member, IEEE*

***Abstract*—This paper presents the Butterworth-van Dyke model and quantitative comparison that explore the design space of lead zirconate titanate-only (PZT) and PZT on 3-, 5-, and 10-μm single-crystal silicon (SCS) high-overtone width-extensional mode (WEM) resonators with identical lateral dimensions for incorporation into radio frequency microelectromechanical systems (RF MEMS) filters and oscillators. A novel fabrication technique was developed to fabricate the resonators with and without a silicon carrier layer using the same mask set on the same wafer. The air-bridge metal routings were implemented to carry electrical signals while avoiding large capacitances from the bond-pads. We theoretically derived and experimentally measured the correlation of motional impedance (R_X), quality factor (Q), and resonance frequency (f) with the resonators' silicon layer thickness (t_{Si}) up to frequencies of operation above 1 GHz.**

I. Introduction

The development of modern integrated wireless communication systems has pushed the investigation of efficient electromechanical transducer materials for microelectromechanical resonators and filters. Ferroelectric materials such as lead zirconate titanate (PZT) are favorable transducers for devices that operate at high frequencies up to the UHF range because they avoid thick film requirements and reduce the area required for the resonators and filters. Furthermore, PZT exhibits a large electromechanical coupling coefficient, enabling the design of larger percentage bandwidth filters [1].

PZT is also an attractive electromechanical transducer because it possesses a dc bias-dependent elastic modulus. This property has been utilized to design PZT transduced length-extensional mode (LEM) resonators with up to 5% frequency tuning [2]. However, PZT-only resonators are well known to have low Q. To overcome the low Q of PZT-only resonators, we have developed a new fabrication technology to integrate PZT transduction with single-crystal silicon (SCS) resonators. This fabrication technology allows us to fabricate PZT-only and PZT-on-silicon resonators using the same mask set on the same wafer.

Manuscript received January 5, 2010; accepted June 18, 2010.

H. Chandrahalim was with the School of Electrical and Computer Engineering, Cornell University, Ithaca, NY. He is now with the Micro and Nanosystems Laboratory, Swiss Federal Institute of Technology, Zurich, Switzerland (e-mail: hengky.chandrahalim@micro.mavt.ethz.ch).

S. A. Bhave is with the School of Electrical and Computer Engineering, Cornell University, Ithaca, NY.

R. G. Polcawich, J. S. Pulskamp, and R. Kaul are with the US Army Research Laboratory, Adelphi, MD.

Digital Object Identifier 10.1109/TUFFC.2010.1651

The material properties and piezoelectric coefficient of PZT solely dominate the Butterworth-van Dyke (BVD) model in PZT-only resonators. However, the effective mass, M_{Eff}, effective stiffness, K_{Eff}, and the damping factor, ζ, of PZT-on-silicon resonators are scaled by the ratio of the thickness of the PZT layer, t_{PZT}, to that of the silicon layer, t_{Si}. Several research groups have previously demonstrated aluminum nitride (AlN) and zinc oxide (ZnO) transduction of MEMS resonators with and without a silicon carrier layer and derived the corresponding BVD models [3]–[5]. However, the thicknesses of piezoelectric films in many applications are usually much smaller than the thickness of the silicon carrier layer. Thus, the mass of the thin film transducer can be neglected without affecting the accuracy of the equivalent electrical model very much. In this paper we derive, simulate, and experimentally justify a model that will hold true for any thickness ratio of the piezoelectric transducer and silicon carrier layer. The model converges to models presented in references [3]–[5] for the specific thickness cases.

II. High-Overtone WEM Resonator

PZT-transduced LEM resonators have been successfully demonstrated. By varying the silicon thickness, t_{Si}, (thereby the percent mass of crystalline silicon in the resonator) and dc bias voltage, we can define the desired Q and frequency tuning range of the resonators [2]. However, various applications in wireless communication systems demand higher frequency of operation. To reach f above 100 MHz using the length-extensional mode of vibration, the length of PZT-on-silicon resonators must be scaled down to less than 40 μm. The length of PZT-only resonators must be shrunk even more because of the lower acoustic velocity compared with PZT-on-silicon resonators. Aggressive scaling in lateral dimensions of the resonator reduces the transduction area, resulting in poor motional impedances. To enable PZT-transduced resonators with a high frequency of operation while maintaining low motional impedance, design and fabrication of PZT-transduced high-overtone width-extensional mode (WEM) resonators will be presented.

A. Design of a High-Overtone WEM Resonator

A high-overtone width-extensional mode of vibration can be excited to achieve a high resonance frequency while utilizing a large transduction area [6]. The schematic of

0885–3010/$25.00 © 2010 IEEE

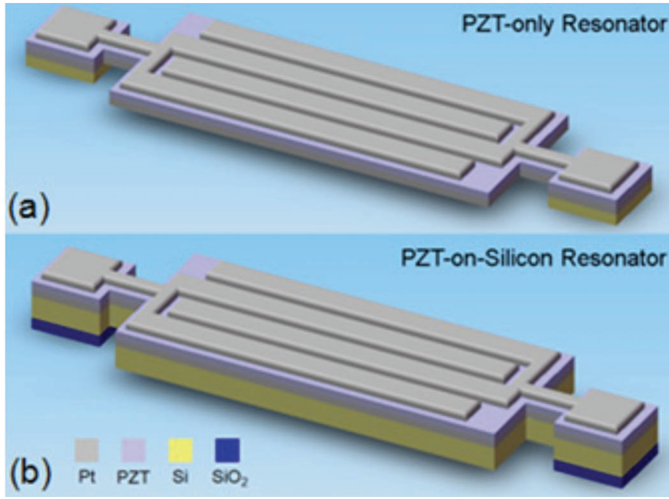

Fig. 1. Schematic of (a) PZT-only resonator and (b) PZT-on-silicon resonator.

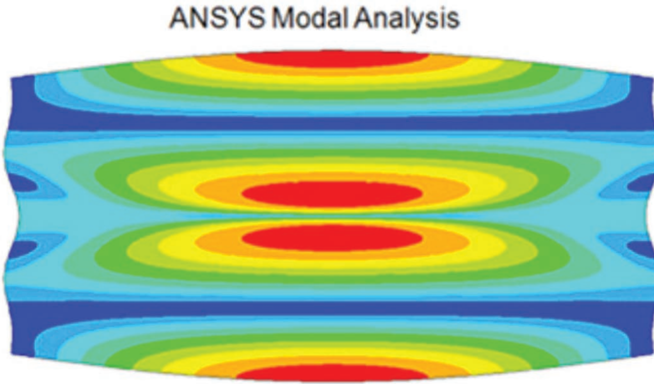

Fig. 2. ANSYS mode shape of a high-overtone width-extensional mode resonator.

PZT-only and PZT-on-silicon resonators are illustrated in Figs. 1(a) and 1(b), respectively. By selectively patterning the interdigitated electrodes on top of the resonators, the higher overtone of width-extensional mode is excited as demonstrated in ANSYS modal analysis (Ansys, Inc., Canonsburg, PA) in Fig. 2.

B. Effective Mass, Damping Ratio, and Effective Spring Constant

The cross-sectional view of a WEM resonator with width W and thickness $t_{\mathrm{PZT}} + t_{\mathrm{Si}}$ is shown in Fig. 3. We assume in our analysis and derivation throughout this paper that the structure of our devices is either dominated by PZT layer (t_{PZT}, for PZT-only resonators) or PZT and silicon composite structure ($t_{\mathrm{PZT}} + t_{\mathrm{Si}}$, for PZT-on-silicon resonators). Though the strain is assumed to be uniform in the x-, y-, and z-directions, we designed all suspensions of the resonators to strongly excite the width-extensional mode of vibrations. Because the displacement normal to the x-direction is presumed to be negligibly small, the three-dimensional equation of motion can be reduced into a one-dimensional model. The resonator vibrates in the direction normal to area A (not shown in the picture).

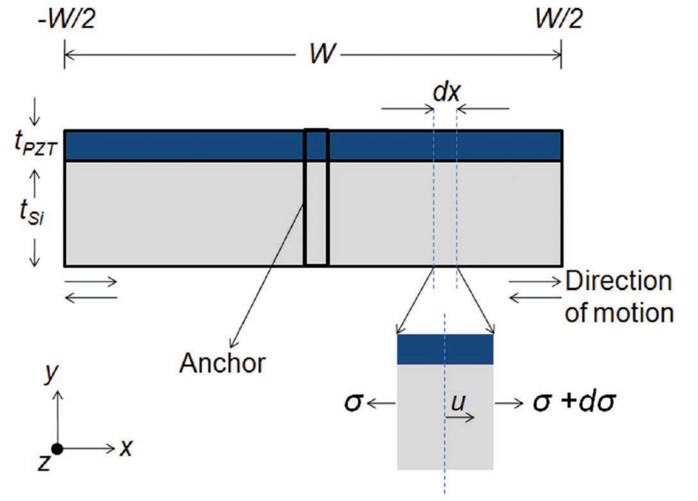

Fig. 3. The cross-sectional view of a width-extensional mode resonator.

From Newton's law of motion, the sum of forces that act on the resonator can be expressed as

$$(\sigma(x,t) + d\sigma(x,t))A - \sigma(x,t)A = \rho_{\mathrm{Eff}} A\, dx \frac{\partial^2 u(x,t)}{\partial t^2}, \quad (1)$$

where u and σ are the displacement of center mass and the distributed stress across the thickness of the composite resonator, respectively. Eq. (1) can be simplified as

$$A\frac{\partial \sigma(x,t)}{\partial x} = \rho_{\mathrm{Eff}} A \frac{\partial^2 u(x,t)}{\partial t^2} \quad (2)$$

$$A\frac{\partial E_{\mathrm{Eff}} \frac{\partial u(x,t)}{\partial x}}{\partial x} = \rho_{\mathrm{Eff}} A \frac{\partial^2 u(x,t)}{\partial t^2} \quad (3)$$

$$E_{\mathrm{Eff}} A \frac{\partial^2 u(x,t)}{\partial x^2} = \rho_{\mathrm{Eff}} A \frac{\partial^2 u(x,t)}{\partial t^2}, \quad (4)$$

where E_{Eff} and ρ_{Eff} are the effective two-dimensional elastic modulus and density of the composite resonator, respectively.

The wave equation for a one-dimensional vibrating width-extensional mode resonator including the damping factor, b and external forces, $f(x, t)$ is

$$\rho_{\mathrm{Eff}} A \frac{\partial^2 u}{\partial t^2}(x,t) - bA\frac{\partial}{\partial t}\frac{\partial^2 u}{\partial x^2}(x,t) - E_{\mathrm{Eff}} A \frac{\partial^2 u}{\partial x^2}(x,t) = \frac{\partial f}{\partial x}(x,t). \quad (5)$$

By the method of separation of variables, we assume (5) has solutions of the form

$$u(x,t) = g(t)\sin\left(\frac{n\pi}{W}x\right), \quad (6)$$

where $g(t)$ is the vibration amplitude as a function of time. Substituting (6) into (5) gives

$$\rho_{\text{Eff}} A \sin\left(\frac{n\pi}{W}x\right)\frac{\partial^2 g(t)}{\partial t^2} + bA\left(\frac{n\pi}{W}\right)^2 \sin\left(\frac{n\pi}{W}x\right)\frac{\partial g(t)}{\partial t} + E_{\text{Eff}} A\left(\frac{n\pi}{W}\right)^2 \sin\left(\frac{n\pi}{W}x\right)g(t) = \frac{\partial f}{\partial x}(x,t). \tag{7}$$

Multiply (7) by $\sin(((n\pi)/W)x)$ and integrate over the width to yield

$$\int_{-W/2}^{W/2}\left[\rho_{\text{Eff}} A\left(\sin\left(\frac{n\pi}{W}x\right)\right)^2 \frac{\partial^2 g(t)}{\partial t^2} + bA\left(\frac{n\pi}{W}\right)^2\left(\sin\left(\frac{n\pi}{W}x\right)\right)^2\frac{\partial g(t)}{\partial t} + E_{\text{Eff}} A\left(\frac{n\pi}{W}\right)^2\left(\sin\left(\frac{n\pi}{W}x\right)\right)^2 g(t)\right]\mathrm{d}x = F(t), \tag{8}$$

where

$$F(t) = \int_{-W/2}^{W/2}\frac{\partial f}{\partial x}\sin\left(\frac{n\pi}{W}x\right)\mathrm{d}x$$

is the time dependent excitation force.

Eq. (8) can be simplified as

$$\frac{\rho_{\text{Eff}} A W}{2}\frac{\partial^2 g(t)}{\partial t^2} + \frac{bAW}{2}\left(\frac{n\pi}{W}\right)^2\frac{\partial g(t)}{\partial t} + \frac{E_{\text{Eff}} A W}{2}\left(\frac{n\pi}{W}\right)^2 g(t) = F(t). \tag{9}$$

From (9), we can recognize that the effective mass, damping ratio, and effective spring constant of a width-extensional mode resonator with width W are given by

$$M_{\text{Eff}} = \frac{\rho_{\text{Eff}} A W}{2} \tag{10}$$

$$\zeta = \frac{bAW}{2}\left(\frac{n\pi}{W}\right)^2 = \frac{n^2 bA\pi^2}{2W} \tag{11}$$

$$K_{\text{Eff}} = \frac{E_{\text{Eff}} A W}{2}\left(\frac{n\pi}{W}\right)^2 = \frac{n^2 E_{\text{Eff}} A\pi^2}{2W}. \tag{12}$$

C. Effective Elastic Modulus and Density

The piezoelectric force induced by the PZT layer is distributed along the thickness of the composite resonator ($t_{\text{Si}} + t_{\text{PZT}}$). The uniform displacement along the thickness of the composite resonator leads into the average strain, ε_{Eff}.

$$\varepsilon_{\text{Eff}} = \frac{\Delta W}{W}, \tag{13}$$

where ΔW is the amount of change in static width caused by time-dependent excitation force $F(t)$. Because of the elastic properties of PZT and silicon layers, the stress components of PZT and silicon are

$$\sigma_{\text{PZT}} = E_{\text{PZT}}\varepsilon_{\text{Eff}} \tag{14}$$

and

$$\sigma_{\text{Si}} = E_{\text{Si}}\varepsilon_{\text{Eff}}, \tag{15}$$

where E_{PZT} and E_{Si} are the two-dimensional elastic moduli of PZT and silicon, respectively. The average stress, σ_{Eff} acts on the cross-sectional area, A, of the composite resonator which is orthogonal to the direction of motion. This average stress yields an effective force, F_{Eff}, on the composite resonator

$$F_{\text{Eff}} = \sigma_{\text{Eff}} A = \sigma_{\text{PZT}} A_{\text{PZT}} + \sigma_{\text{Si}} A_{\text{Si}}. \tag{16}$$

By substituting (16) with (14) and (15), we obtain

$$\sigma_{\text{Eff}} A = E_{\text{PZT}}\, \varepsilon_{\text{Eff}}\, A_{\text{PZT}} + E_{\text{Si}}\, \varepsilon_{\text{Eff}}\, A_{\text{Si}}. \tag{17}$$

The effective two-dimensional elastic modulus, E_{Eff} is obtained by dividing σ_{Eff} in (17) by ε_{Eff}:

$$E_{\text{Eff}} = \frac{t_{\text{PZT}} E_{\text{PZT}} + t_{\text{Si}}\, E_{\text{Si}}}{t_{\text{PZT}} + t_{\text{Si}}}. \tag{18}$$

We assume the length of the PZT transducer, L_{PZT}, in our device is approximately the same as the length of the silicon carrier layer, L_{Si}. By using the same line of derivation, the effective density, ρ_{Eff}, of the composite resonator is given by

$$\rho_{\text{Eff}} = \frac{t_{\text{PZT}}\rho_{\text{PZT}} + t_{\text{Si}}\rho_{\text{Si}}}{t_{\text{PZT}} + t_{\text{Si}}}. \tag{19}$$

D. Electromechanical Transduction Efficiency

The lateral stress, σ_{PZT} in the PZT film is given by

$$\sigma_{\text{PZT}} = e_{31}\frac{v_{\text{AC}}}{t_{\text{PZT}}}, \tag{20}$$

where e_{31} and t_{PZT} are the transverse piezoelectric stress constant and thickness of PZT layer, respectively, and v_{AC} is the time-dependent actuation voltage.

By substituting e_{31} with $d_{31} \times E_{\text{PZT}}$, (20) can be written as

$$\sigma_{\text{PZT}} = d_{31} E_{\text{PZT}}\frac{v_{\text{AC}}}{t_{\text{PZT}}}, \tag{21}$$

where d_{31} and E_{PZT} are the transverse piezoelectric coefficient and two-dimensional elastic modulus of PZT, respectively. The generated piezoelectric force, $F_{\text{PZT}}|_{W/2}$ caused by PZT transduction at $W/2$ can be obtained by multi-

plying the generated stress with the cross-sectional area of the PZT film which is orthogonal to direction of motion:

$$F_{\mathrm{PZT}}\big|_{W/2} = \sigma_{\mathrm{PZT}} A_{\mathrm{PZT}} = d_{31}\, E_{\mathrm{PZT}} L v_{\mathrm{AC}}. \quad (22)$$

We assume the length of the PZT transducer, L_{PZT}, in our device is approximately the same as the length of the silicon carrier layer, L_{Si}, and is denoted by L in (22). Because of the width-extensional boundary condition that was imposed to excite the resonator, the same piezoelectric force, $F_{\mathrm{PZT}}|_{-W/2}$ with opposite direction exists at $-W/2$. The efficiency of electromechanical transduction by PZT is indicated by the electromechanical transduction efficiency, η; η is the ratio of the total generated piezoelectric force, F_{PZT}, to the applied time varying voltage, v_{AC}:

$$\eta = \frac{F_{\mathrm{PZT}}}{v_{\mathrm{AC}}} = 2\, d_{31} E_{\mathrm{PZT}} L. \quad (23)$$

E. Small-Signal Electrical Equivalent Circuit

The effective mass, damping ratio, and effective spring constant can be related to the electrical circuit parameters. In the process of electromechanical transduction, the time-dependent voltage v_{AC} generates a lateral force, F_{PZT}, through the transverse piezoelectric stress constant, e_{31}. The dynamic force F_{PZT} excites acoustic vibrations with amplitude $g(t)$. The charge modulation in the PZT layer due to vibration velocity $\partial g(t)/\partial t$ induces a motional current output, $i(t)$. The relation between time-dependent input stimulus v_{AC} and $i(t)$ can be expressed mathematically as

$$i(t) = \frac{\partial g(t)}{\partial t}\eta. \quad (24)$$

By substituting $\partial g(t)/\partial t$ in (9) by $i(t)/\eta$, we obtain

$$\frac{M_{\mathrm{Eff}}}{\eta}\frac{\partial i(t)}{\partial t} + \frac{\zeta}{\eta} i(t) + \frac{K_{\mathrm{Eff}}}{\eta}\int i(t)\mathrm{d}t = F(t) \quad (25)$$

or

$$\frac{M_{\mathrm{Eff}}}{\eta^2}\frac{\partial i(t)}{\partial t} + \frac{\zeta}{\eta^2} i(t) + \frac{K_{\mathrm{Eff}}}{\eta^2}\int i(t)\mathrm{d}t = v_{\mathrm{AC}}(t). \quad (26)$$

From (26), we can define the motional resistance, capacitance, and inductance of the 2-port PZT-on-silicon composite resonator. They are normally represented in parallel with the feedthrough capacitance C_{ft}, as shown in Fig. 4. For a given transduction efficiency η, $R_X = \zeta/\eta^2$, $C_X = \eta^2/K_{\mathrm{Eff}}$, and $L_X = M_{\mathrm{Eff}}/\eta^2$. The feedthrough capacitance in a two-port resonator originates from electric field coupling from the input electrode to the output electrode and is a function of electrode geometry. The nominal capacitance, C_0, is the static capacitance between the electrode and the resonator's body. A high-overtone width-extensional mode resonator can be treated as an array of smaller width-extensional mode resonators connected in parallel. Thus,

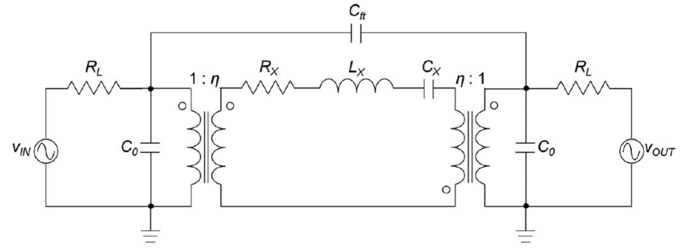

Fig. 4. Electrical equivalent circuit of a PZT-transduced high-overtone WEM resonator, including the static capacitance between the electrode and resonator's body, C_0, the feedthrough capacitance between input and output ports, C_{ft}, and the termination impedance, R_L.

the small signal electrical equivalent impedances of a resonator consist of j number of WEM resonators with width W vibrating in fundamental mode ($n = 1$) connected in parallel are

$$R_X = \frac{\pi}{j4Q}\frac{{\rho_{\mathrm{Eff}}}^{1/2}{E_{\mathrm{Eff}}}^{1/2}}{{E_{\mathrm{PZT}}}^2}\frac{\left(t_{\mathrm{Si}} + t_{\mathrm{PZT}}\right)}{L}\frac{1}{{d_{31}}^2} \quad (27)$$

$$C_X = \frac{4}{j\pi^2}\frac{LW}{(t_{\mathrm{Si}} + t_{\mathrm{PZT}})}\frac{{E_{\mathrm{PZT}}}^2}{E_{\mathrm{Eff}}}{d_{31}}^2 \quad (28)$$

$$L_X = \frac{j}{4}\frac{\rho_{\mathrm{Eff}}}{{E_{\mathrm{PZT}}}^2}\frac{(t_{\mathrm{Si}} + t_{\mathrm{PZT}})W}{L}\frac{1}{{d_{31}}^2}, \quad (29)$$

where Q is the mechanical quality factor of the resonator. Using the identical line of derivation, the motional resistance, capacitance, and inductance of the 2-port PZT-only transduced resonator are given by

$$R_X = \frac{\pi}{j4Q}\frac{{\rho_{\mathrm{PZT}}}^{1/2}}{{E_{\mathrm{PZT}}}^{3/2}}\frac{t_{\mathrm{PZT}}}{L_{\mathrm{PZT}}}\frac{1}{{d_{31}}^2} \quad (30)$$

$$C_X = \frac{4}{j\pi^2}\frac{L_{\mathrm{PZT}}W}{t_{\mathrm{PZT}}}E_{\mathrm{PZT}}{d_{31}}^2 \quad (31)$$

$$L_X = \frac{j}{4}\frac{\rho_{\mathrm{PZT}}}{{E_{\mathrm{PZT}}}^2}\frac{t_{\mathrm{PZT}}W}{L_{\mathrm{PZT}}}\frac{1}{{d_{31}}^2}, \quad (32)$$

which are the small-signal electrical equivalent impedances of piezo-only resonators presented in [3]. The resonant frequency f is given by

$$f = \frac{1}{2\pi}\frac{1}{\sqrt{C_X L_X}}. \quad (33)$$

III. Fabrication Process

The device fabrication is largely based on the fabrication sequence outlined in [2] with additional improvements in the process to eliminate the pad capacitances. PZT is well known to have a large permittivity that can lead to large pad capacitances. Therefore, in this refined fabrication process, air-bridge metal routings were implemented to carry electrical signals while avoiding large capacitances from the bond-pads. In addition, a novel fabrication

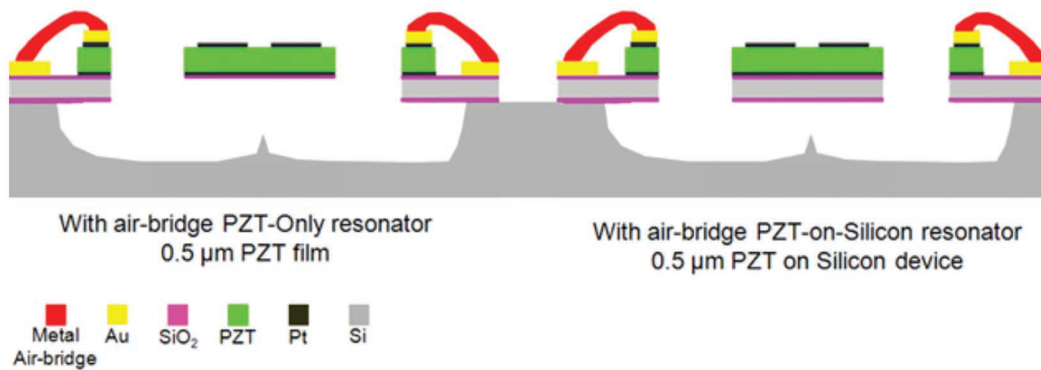

Fig. 5. Air-bridge process cross-section of PZT-only and PZT-on-silicon high-overtone width-extensional mode resonators fabricated on the same wafer.

technique was developed to fabricate the resonators with and without silicon layer using the same mask set on the same wafer. A systematic study is essential to investigate the effect of silicon on Q, f, and R_X of PZT-transduced resonators at radio frequency. In this research effort, we fabricated PZT-only and PZT on 3-, 5-, and 10-µm SCS high-overtone width-extensional mode resonators with identical lateral dimensions.

A PZT transducer comprised of Ti/Pt/PZT/Pt were deposited on SOI wafers with 3-, 5-, and 10-µm thick device layer. The 0.5-µm thick PZT films were deposited using a chemical solution deposition method with a crystallization temperature of 700°C to achieve full densification and high crystallinity. The input and output terminals of the resonators are lithographically defined by patterning the top Pt electrode on top of the PZT actuator. The current configuration of the resonator uses a common bottom Pt electrode underneath the PZT for both the input and output ports. The process cross-section of released PZT-on-silicon and PZT-only resonators is shown in Fig. 5. To ensure survival of the single-crystal silicon component of the resonators, an organic photo-definable layer was developed to provide protection of the resonator while allowing undercutting of the handle silicon wafer using a XeF_2 etch. At the end of device fabrication, the PZT film already possesses some degree of poling as a result of the plasma processing. To improve the degree of poling, the resonators were subjected to electric fields of 200 kV/cm for 10 min before testing. An SEM image of the fabricated high-overtone width-extensional mode resonator is shown in Fig. 6.

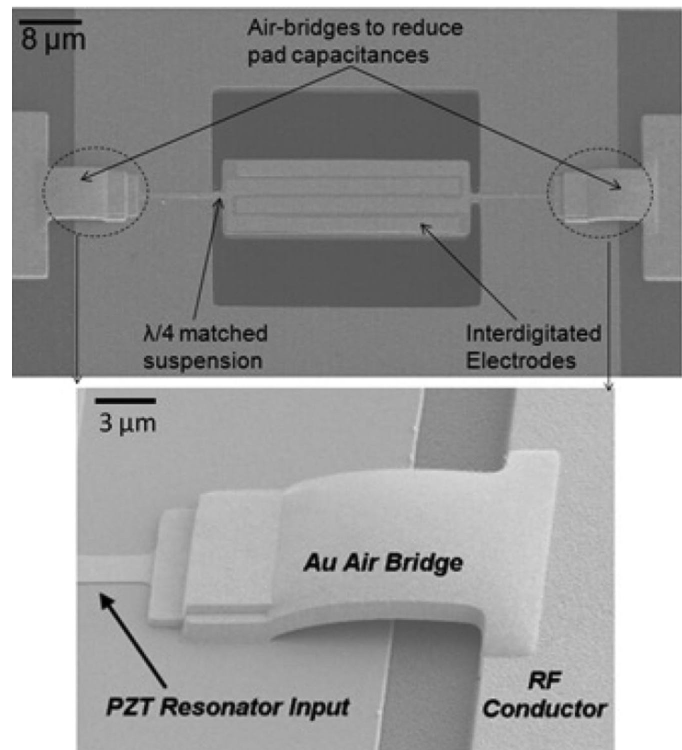

Fig. 6. SEM image of the fabricated high-overtone width-extensional mode resonator. The close-up picture shows the air-bridge routing that isolates the resonator from the bonding-pads.

IV. Characterization of High-Overtone WEM Resonators

The resonators were characterized in an RF probe station in a 2-port configuration using GSG probes. Parasitics up to the probe tips were first calibrated with SOLT measurements on a standard calibration substrate. All measurements were performed in air, at room temperature and pressure. The measurement setup is presented in Fig. 7. The trade-offs in Q, f, and R_X of resonators with different silicon thicknesses were recorded. Resonators with thicker silicon layer exhibit higher Q, higher f, and lower R_X for frequency up to about 900 MHz as shown in Fig. 8. The measured characteristics of the second-overtone WEM resonators with different silicon thicknesses are summarized in Table I. Table II compares the analytically estimated motional inductance and capacitance of second-overtone WEM resonators with the experimentally extracted data. The maximum variation between theoretical and measured data is less than 9%.

The measured resonance frequency of the resonators with different silicon thicknesses are in agreement with the theoretically analyzed and simulated data. Fig. 9 plotted

TABLE I. The Measured Characteristics of High-Overtone WEM Resonators With Different Silicon Thicknesses.

	t_{Si} (µm)			
	0	3	5	10
Q_{Loaded}	150	314	501	458
f (MHz)	428	834	942	1018
R_X (Ω)	390	296	435	700
R_L (Ω)	50	50	50	50
$f \times Q$	6.4×10^{10}	2.6×10^{11}	4.6×10^{11}	4.7×10^{11}

TABLE II. LC Tank of High-Overtone WEM Resonators: Design and Measurement Summary.

	Designed			Measured		
t_{Si} (µm)	L_X (µH)	C_X (fF)	f (MHz)	L_X (µH)	C_X (fF)	f (MHz)
0	84.5	1.820	406	80.1	1.730	428
3	244	0.130	893	261	0.140	834
5	350	0.080	949	353	0.081	942
10	616	0.041	1000	560	0.037	1018

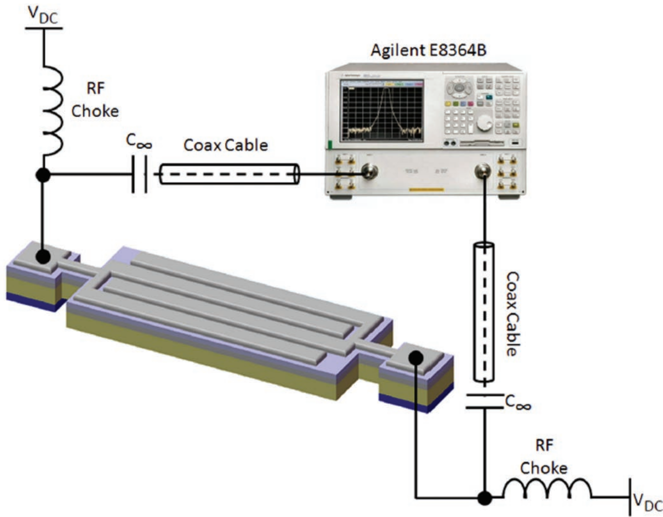

Fig. 7. Testing configuration for a PZT-transduced high-overtone width-extensional mode resonator.

the calculated, simulated, and measured resonance frequency of PZT transduced second-overtone WEM resonators with different silicon thicknesses (t_{Si}). By integrating PZT transduction with single-crystal silicon, the figure of merit, $f \times Q$, is improved by one order of magnitude.

V. Conclusion

In conclusion, we have fabricated PZT transduced high-overtone WEM resonators with and without a silicon device layer using the same mask on the same wafer. A novel fabrication technique has been developed to allow cancelation of large pad capacitances. The BVD models for PZT-only and PZT-on-silicon high-overtone WEM resonators have been derived and used to design resonators with frequency above 1 GHz. The performances of PZT transduced high-overtone WEM resonators with various silicon thicknesses were investigated. Integrating PZT transduction with silicon improves the $f \times Q$ by one order of magnitude. Frequency of operation is dominated by the silicon layer for silicon thickness larger than 3 µm. By varying the silicon thickness, we can define the desired Q and center frequency of the resonators from high frequency up to the ultra high frequency range. This technology will enable PZT-transduced resonators, filters, and oscillators that cover the range up to low-band GSM frequencies.

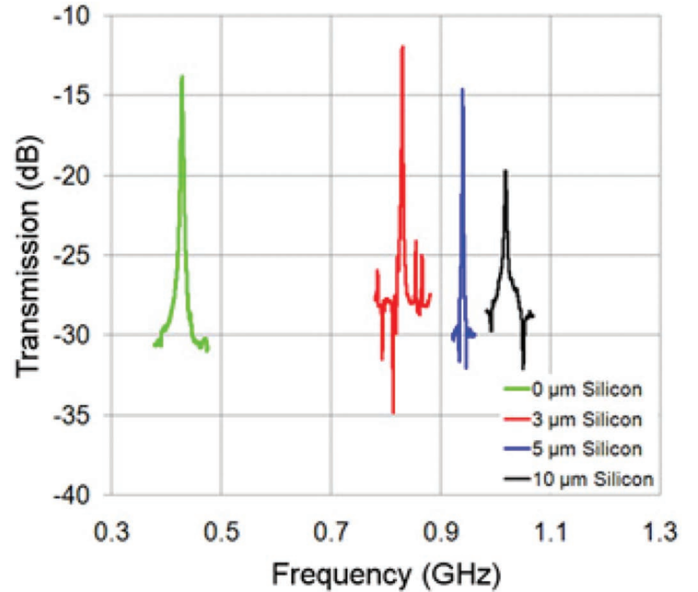

Fig. 8. Measured transmission response of PZT-only and PZT on 3-, 5-, and 10-µm silicon WEM second-overtone resonators with the exact same lateral dimensions in air at room temperature and pressure. All measurements were performed using termination impedances (R_L) of 50 Ω.

Acknowledgment

The authors would like to thank B. Power, J. Martin, and R. Piekarz of the Army Research Laboratory for their assistance in fabricating the resonators.

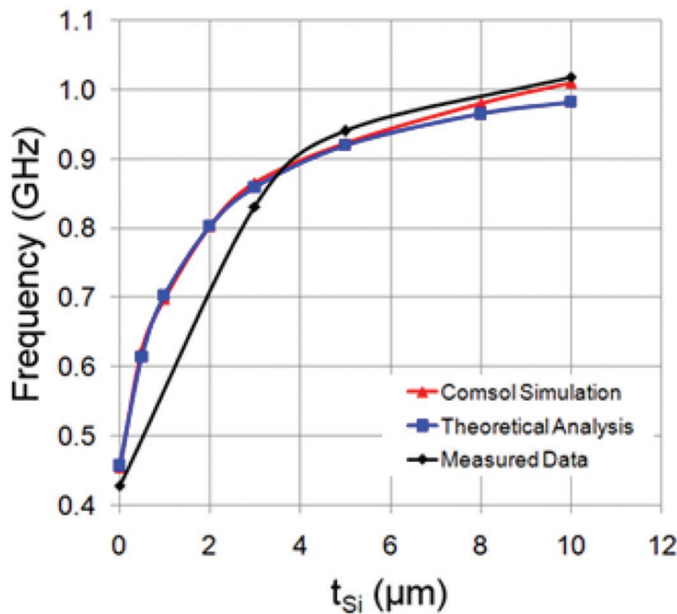

Fig. 9. A plot of silicon thickness (t_{Si}) versus the calculated, simulated, and measured resonance frequency (f).

References

[1] J. D. Larson, III, S. R. Gilbert, and B. Xu, "PZT material properties at UHF and microwave frequencies derived from FBAR measurements," in *Proc. IEEE Ultrasonics Symp.*, Montreal, Canada, 2004, vol. 1, pp. 173–177.

[2] H. Chandrahalim, S. A. Bhave, R. Polcawich, J. Pulskamp, D. Judy, R. Kaul, and M. Dubey, "Performance comparison of $Pb(Zr_{0.52}Ti_{0.48})O_3$-only and $Pb(Zr_{0.52}Ti_{0.48})O_3$-on-silicon resonators," *Appl. Phys. Lett.*, vol. 93, no. 23, art. no. 233504, 2008.

[3] G. Piazza, P. J. Stephanou, and A. P. Pisano, "Piezoelectric aluminum nitride vibrating contour-mode MEMS resonators," *J. Microelectromech. Syst.*, vol. 15, no. 6, pp. 1406–1418, 2006.

[4] G. K. Ho, R. Abdolvand, A. Sivapurapu, S. Humad, and F. Ayazi, "Piezoelectric-on-silicon lateral bulk acoustic wave micromechanical resonators," *J. Microelectromech. Syst.*, vol. 17, no. 2, pp. 512–520, 2008.

[5] A. Jaakkola, P. Rosenberg, A. Nurmela, T. Pensala, T. Riekkinen, J. Dekker, T. Mattila, and A. Alastalo, "Piezotransduced single-crystal silicon BAW resonators," in *Proc. IEEE Ultrasonics Symp.*, New York, NY, 2007, pp. 1653–1656.

[6] G. K. Ho, R. Abdolvand, and F. Ayazi, "High-order composite bulk acoustic resonators," in *Proc. IEEE Int. Conf. Micro Electro Mechanical Systems (MEMS)*, Kobe, Japan, 2007, pp. 791–794.

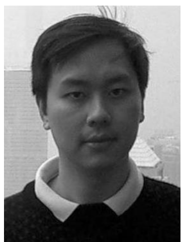

Hengky Chandrahalim (S'04–M'09) completed his undergraduate education with the B.S. degree in electrical and computer engineering from the Ohio State University. He received his Ph.D. degree in electrical and computer engineering from Cornell University in 2009 with research focus in voltage tunable radio frequency micro-electromechanical resonators and filters. Dr. Chandrahalim worked as an integrated circuit design engineer at Integrated Circuit Systems, Inc. in San Jose, CA, from 2000 to 2003. Soon after his graduation from Cornell University, Dr. Chandrahalim joined the Micro and Nanosystems laboratory at ETH Zurich as a postdoctoral research associate. His current research focus is in carbon-nanotubes-based nano-electromechanical signal processors. Dr. Chandrahalim was the recipient of the IEEE Ultrasonics, Ferroelectrics, and Frequency Control Society 2009 Student Best Paper Award.

Sunil A. Bhave (S'99–M'04–SM'10) received the B.S. and Ph.D. degrees in electrical engineering and computer sciences from the University of California, Berkeley in 1998 and 2004, respectively. In 2004, he joined the faculty of Cornell University, where he is currently an Assistant Professor in the School of Electrical and Computer Engineering. His research interests include MEMS resonators for radios, merged CMOS-NEMS, inertial and acoustic sensors, and hybrid photonic-NEMS and magnetic-NEMS for low-phase-noise microwave oscillators. Professor Bhave is a recipient of the NSF Early CAREER Development Award in 2007 and the DARPA Young Faculty Award in 2008. Together with his students, he has received the Best Paper awards at IEDM 2007 and Ultrasonics 2009.

Ronald G. Polcawich (M'07) received the B.S. in materials science and engineering from Carnegie-Mellon University, Pittsburgh, PA, in 1997, and the M.S. and Ph.D. degrees in materials from The Pennsylvania State University, University Park, in 1999 and 2007, respectively. He is a staff researcher in the Micro & Nano Materials & Devices Branch of the US Army Research Laboratory (ARL), Adelphi, MD. He is currently the team lead for the RF MEMS and Millimeter-Scale Robotics programs at ARL. His research activities include materials processing of PZT thin films, MEMS fabrication, piezoelectric MEMS, RF components, MEMS actuators, and millimeter-scale robotics. Dr. Polcawich is a member of the Materials Research Society and IEEE.

Jeffrey S. Pulskamp received the B.S. degree in mechanical engineering from the University of Maryland at College Park, in 2000. He is currently a Mechanical Engineer with the Advanced MicroDevices Branch, Adelphi Laboratory Center, U.S. Army Research Laboratory, Adelphi, MD. His current research focuses on RF MEMS devices, electronic scanning antenna, mechanical modeling of MEMS, and microrobotics.

Roger Kaul (S'60–M'62–SM'88–SLM'06) received the Ph.D. degree in electrical engineering and applied sciences from Case Western Reserve University, Cleveland, OH, in 1969. Until 1974, he researched Gunn instabilities at the United Aircraft Research Laboratories. He then joined ORI Inc. and performed space system studies for the National Aeronautics and Space Administration (NASA). From 1981 to 1987, he conducted studies related to electronic warfare and millimeter-wave communication systems with the Amecom Division, Litton. Until 2001, he was involved with the development of microwave hardening technology techniques and evaluating microwave devices and circuits for Army applications at the Army Research Laboratory (ARL). He continues to assist the ARL in the development and evaluation of microelectromechanical systems (MEMS) technology as a member of the ARL Emeritus Corps. He is a Part-Time Instructor with the Whiting School of Engineering, Johns Hopkins University, Baltimore, MD. Dr. Kaul is past chair of the MTT-16 Microwave Systems Technical Committee and remains active in the Washington DC/Northern Virginia Chapter of the IEEE Microwave Theory and Techniques Society (IEEE MTT-S).